Validation of ^{18}F-rhPSMA-7 and ^{18}F-rhPSMA-7.3 PET Imaging Results with Histopathology from Salvage Surgery in Patients with Biochemical Recurrence of Prostate Cancer

Markus Kroenke[1,2], Lilit Schweiger[1,3], Thomas Horn[4], Bernhard Haller[5], Kristina Schwamborn[6], Alexander Wurzer[1,7], Tobias Maurer[8], Hans-Jürgen Wester[7], Matthias Eiber*[1,3], and Isabel Rauscher*[1,3]

[1]Department of Nuclear Medicine, School of Medicine, Technical University of Munich, Munich, Germany; [2]Department of Radiology and Nuclear Medicine, German Heart Center Munich, Technical University of Munich, Munich, Germany; [3]Bavarian Cancer Research Center (BZKF), Munich, Germany; [4]Department of Urology, School of Medicine, Technical University of Munich, Munich, Germany; [5]Institute of Medical Informatics, Statistics and Epidemiology, School of Medicine, Technical University of Munich, Munich, Germany; [6]Department of Pathology, School of Medicine, Technical University of Munich, Munich, Germany; [7]Chair of Radiopharmacy, School of Medicine, Technical University of Munich, Munich, Germany; and [8]Martini-Klinik and Department of Urology, University Hospital Hamburg-Eppendorf, Hamburg, Germany

^{18}F-rhPSMA-7, and its single diastereoisomer form, ^{18}F-rhPSMA-7.3, are prostate-specific membrane antigen (PSMA)–targeting radiopharmaceuticals. Here, we investigated their accuracy for the assessment of lymph node (LN) metastases validated by histopathology. **Methods:** Data from 58 patients with biochemical recurrence of prostate cancer after radical prostatectomy receiving salvage surgery after PET imaging with ^{18}F-rhPSMA-7 or ^{18}F-rhPSMA-7.3 were retrospectively reviewed. Two nuclear medicine physicians reviewed all PET scans and morphologic imaging in consensus. Readers were masked from the results of histopathology. PET and morphologic imaging were correlated with histopathology from resected LNs. **Results:** In 75 of 150 resected regions in 54 of 58 patients, tumor lesions were present in histopathology. The template-based specificity of PET (^{18}F-rhPSMA-7 and ^{18}F-rhPSMA-7.3 combined) and morphologic imaging was 93.3% and 100%, respectively. However, ^{18}F-rhPSMA-7 and ^{18}F-rhPSMA-7.3 PET detected metastases in 61 of 75 histopathologically proven metastatic LN fields (81.3%) whereas morphologic imaging was positive in only 9 of 75 (12.0%). The positive predictive value was 92.4% for ^{18}F-rhPSMA-7 and ^{18}F-rhPSMA-7.3 PET and 100% for morphologic imaging. ^{18}F-rhPSMA-7 and ^{18}F-rhPSMA-7.3 PET performance was significantly superior to morphologic imaging (difference in the areas under the receiver-operating-characteristic curves, 0.222; 95% CI, 0.147–0.298; $P < 0.001$). The mean size of PET-positive and histologically confirmed LN metastases was 6.3 ± 3.1 mm (range, 2–15 mm) compared with a mean size of 9.8 ± 2.5 mm (range, 7–15 mm) on morphologic imaging. **Conclusion:** ^{18}F-rhPSMA-7 and ^{18}F-rhPSMA-7.3 PET offer a high positive predictive value comparable to that reported for ^{68}Ga-PSMA-11 and represent a valuable tool for guiding salvage lymphadenectomy.

Key Words: ^{18}F-rhPSMA-7; ^{18}F-rhPSMA-7.3; prostate cancer; salvage surgery; biochemical recurrence; prostate-specific membrane antigen

J Nucl Med 2022; 63:1809–1814
DOI: 10.2967/jnumed.121.263707

Up to one third of all patients with prostate cancer (PC) will experience biochemical recurrence after initial curative-intended treatment (*1*). Salvage therapies such as salvage surgery and other metastasis-directed treatments can prolong the interval until systemic therapy is needed (*2–4*). To perform any localized treatment, for either metastasis or local recurrence, accurate diagnostic imaging is of utmost importance. Several studies have already proven the superiority of PET targeting the prostate-specific membrane antigen (PSMA) compared with morphologic imaging (e.g., CT and MRI) for localization of recurrent disease or for primary N staging (*5,6*). In this context, ^{68}Ga-PSMA-11 has been the PSMA-ligand most extensively assessed in several retrospective and prospective studies, leading to its approval and recommendation by various guidelines as the preferred imaging tool for restaging (*7–11*).

However, ^{18}F-labeled PSMA-targeting ligands are becoming increasingly used in preference to ^{68}Ga-labeled counterparts because of the principal advantages of radiofluorinated tracers (e.g., longer half-life and large batch production in cyclotrons leading to the possibility of centralized production and distribution as well as lower positron energy of ^{18}F compared with ^{68}Ga) (*12*).

^{18}F-rhPSMA-7 is one such ^{18}F-labeled PSMA-targeting ligand representing a class of radiohybrid PSMA (rhPSMA) ligands that can be labeled with ^{18}F for imaging purposes but also with other radioactive isotopes such as ^{177}Lu for endoradiotherapy (*13*). ^{18}F-rhPSMA-7 is composed of 4 diastereoisomers (^{18}F-rhPSMA-7.1–7.4) (*14*). Of these, ^{18}F-rhPSMA-7.3 was selected for clinical development on the basis of its superior characteristics in preclinical studies, including fast clearance from blood pool, liver, and kidneys as well as high tumor accumulation in LNCaP tumor–bearing mice (*14*). ^{18}F-rhPSMA-7.3 is currently under investigation in 2 multicenter phase III trials for PET imaging (NCT04186845 and NCT04186819); it shows properties similar to those of the isomeric mixture ^{18}F-rhPSMA-7, with both PSMA-ligands demonstrating high detection rates in patients with biochemical recurrence of PC (*15,16*).

However, to date, no histopathology-validated study on the use of ^{18}F-rhPSMA-7.3 in patients with biochemical recurrence of PC has been published. Thus, the aim of this retrospective analysis was to assess the performance of ^{18}F-rhPSMA-7 and ^{18}F-rhPSMA-7.3 PET

Received Dec. 25, 2021; revision accepted Mar. 28, 2022.
For correspondence or reprints, contact Isabel Rauscher (isabel.rauscher@tum.de).
*Contributed equally to this work.
Published online Apr. 7, 2022.

in patients with biochemical recurrence after radical prostatectomy undergoing subsequent salvage surgery for histopathologic comparison.

MATERIALS AND METHODS

Patients

We retrospectively reviewed the institution's database for all patients with biochemical recurrence of PC who underwent either ^{18}F-rhPSMA-7 or ^{18}F-rhPSMA-7.3 PET and subsequent salvage surgery between November 2017 and June 2020. Patients were excluded if they had not undergone radical prostatectomy as a primary treatment. In total, 58 patients were identified. The retrospective analysis was approved by the local ethics committee (permit 290/18S and 99/19). Administration of ^{18}F-rhPSMA-7 and ^{18}F-rhPSMA-7.3 complied with the German Medicinal Products Act, AMG §13 2b, and the responsible regulatory body (government of Oberbayern).

^{18}F-rhPSMA Synthesis, Administration, and PET Imaging

^{18}F-rhPSMA-7 and ^{18}F-rhPSMA-7.3 were synthesized and used as previously reported (*13,17,18*). Twenty-three (40%) patients received ^{18}F-rhPSMA-7, and 35 (60%) patients received the single-isomer ^{18}F-rhPSMA-7.3. ^{18}F-rhPSMA-7 and ^{18}F-rhPSMA-7.3 were administered (median activity, 320 MBq; range, 239–399 MBq) as an intravenous bolus a median of 72 min (range, 60–148 min) before scanning. In total, 49 patients underwent contrast-enhanced PET/CT (Biograph mCT Flow [Siemens Healthineers]; contrast agent: Imeron 300 [Bracco Imaging]), and 9 patients underwent PET/MRI (Biograph mMR; Siemens Healthineers). The fully diagnostic PET/CT and PET/MRI examinations were conducted as previously reported (*19,20*). Furosemide (20 mg intravenously) was administered to all patients at the time of tracer application, and patients were asked to void urine before the scan.

All PET/CT scans were acquired in 3-dimensional mode with time of flight and in continuous table motion (flowMotion technology, Siemens (*21*)) with 1.1 mm/s, equal to 2 min per bed position. The PET/MRI scans were acquired in 3-dimensional mode and step-and-shoot with 4 min per bed position for PET/MRI. Emission data were corrected for randoms, dead time, scatter, and attenuation and were reconstructed iteratively by an ordered-subsets expectation maximization algorithm (4 iterations, 8 subsets) followed by a postreconstruction smoothing gaussian filter (5 mm in full width at half maximum).

Image Analysis

All ^{18}F-rhPSMA-7 and ^{18}F-rhPSMA-7.3 PET/CT and PET/MRI datasets were reviewed by *2* experienced board-certified nuclear medicine specialists in consensus. The readers were masked to the results of histopathology. First, the CT dataset of the PET/CT or the dedicated high-resolution axial T2-weighted turbo spin echo sequence of the pelvis up to the aortic bifurcation (slice thickness, 5 mm each) of the PET/MRI were analyzed. Second, after an interval of at least 4 wk, the corresponding ^{18}F-rhPSMA-7 and ^{18}F-rhPSMA-7.3 PET scans were read by the same readers, with the morphologic imaging only being used for anatomic allocation. Findings were rated using a 5-point Likert scale as described previously (*22*): PET rating of 5 indicates a tumor manifestation (intense, focal uptake, uptake higher than in the liver); 4, probable tumor manifestation (uptake clearly higher than the background level in vessels but less than in the liver); 3, equivocal findings (faint uptake between muscle and vessels uptake); 2, probable benign findings (uptake equal to the adjacent muscle); 1, benign findings (no uptake).

For both CT and MRI, the same Likert scale was applied with a rating of 5 indicating tumor manifestation (lymph node short-axis diameter $>$ 10 mm); 4, probable tumor manifestation (short-axis diameter of 8–10 mm or a round configuration or a regional grouping); 3, equivocal findings (short-axis diameter of 8–10 mm, an oval configuration, and no regional grouping); 2, probable benign findings (short-axis diameter $<$ 8 mm); and 1, benign findings (short-axis diameter $<$ 5 mm). Finally, SUV_{max} and size (short-axis diameter) of the largest lymph node per template region rated with a score 4 or 5 were measured.

Surgery and Histopathology

The patients were selected for salvage surgery by an interdisciplinary tumor board based on clinical characteristics and the initial clinical reads of ^{18}F-rhPSMA-7 or ^{18}F-rhPSMA-7.3 PET. The salvage surgery was planned based on the information on PET and the surgical fields were limited to the pelvis including potential local recurrence. Depending on the location, adjacent lymph node template regions were resected as well. The lymph node template regions were separately collected. Uropathologists were masked to imaging results.

Statistical Analysis

The histopathologic results from resected lymph nodes were correlated with the results of morphologic imaging (MRI or CT) and ^{18}F-rhPSMA-7 and ^{18}F-rhPSMA-7.3 PET in a patient- and template-based manner. Further, a separate template-based analysis of ^{18}F-rhPSMA-7 and ^{18}F-rhPSMA-7.3 was performed. Results from the 5-point Likert scale were dichotomized to allow estimation of sensitivity, specificity, positive predictive value (PPV), and accuracy. For the statistical analysis, we decided that only scores indicating definitive or probable tumor manifestation on PET and morphologic imaging (scores $\geq$ 4) were counted as positive. This decision was based on a clinical consideration that invasive procedures (e.g., secondary lymphadenectomy and associated general anesthesia) with their potential risks are not justified if only equivocal findings (score 3) are present.

The overall diagnostic accuracy of template-based data was assessed using receiver-operating-characteristic (ROC) analyses. ROC curves were calculated for both modalities. Areas under the ROC curves with 95% CIs were calculated and compared with each other. The approach proposed by Obuchowski was considered for region-based analyses to account for correlations of multiple findings within 1 patient with the help of generalized estimating equations extension of linear regression model (*23*). A significance level of 5% was considered for all tests. All statistical analyses were performed using the statistical software R with its packages pROC and geepack (*24–26*).

RESULTS

Patient Characteristics and Histopathologic Results

The data for 58 patients were reviewed. The patients were a median age of 68.5 y (age range, 51–85 y) and presented with a median prostate-specific antigen (PSA) level of 0.71 ng/mL (range, 0.16–8.39 ng/mL) before the PET scan. Detailed patient characteristics are presented in Table 1. Supplemental Tables 1 and 2 (supplemental materials are available at http://jnm.snmjournals.org) provide detailed per-patient information on patient characteristics, imaging methods, and results.

In 54 of 58 patients, pelvic tumor lesions were confirmed by histopathology. Overall, 150 template regions were resected, with 75 of these harboring tumor lesions (50%). Most (n = 129) were part of the typical pelvic lymph node template. Other resected regions were 9 retroperitoneal locations (n = 6 positive on histopathology) and 12 local regions due to suspicion of local recurrence (n = 10 positive on histopathology).

Imaging Results

The template-based areas under the ROC curves for ^{18}F-rhPSMA-7 and ^{18}F-rhPSMA-7.3 were 0.891 (95% CI, 0.838–0.944) and for morphologic imaging 0.669 (95% CI, 0.595–0.742, Fig. 1). ^{18}F-rhPSMA-7 and ^{18}F-rhPSMA-7.3 PET performed significantly better than morphologic imaging for the detection of lymph node metastases

TABLE 1
Patient Characteristics (n = 58)

Characteristic	Data (%)
Age (y)	
Median	68.5
Range	51–85
iPSA (ng/mL)*	
Median	10.00
Range	1.9–57.9
ISUP grade (*n*)	
1–2	17 (29)
3–4	27 (47)
5	10 (17)
Missing	4 (6.9)
Pathologic T stage at primary RPE (*n*)	
≤pT2c	23 (40)
pT3a	11 (19)
≥pT3b	18 (31)
Missing	6 (10)
Pathologic N stage at primary RPE (*n*)	
pN0	39 (67)
pN1	10 (17)
Missing	9 (16)
Time between primary surgery and PET (mo)	
Median	48
Range	1–278
Prescan PSA (ng/mL)†	
Median	0.71
Range	0.16–8.39
Time between PET and salvage surgery (d)	
Median	59
Range	19–117
Lymph node regions removed at salvage LAE	
N	150
Median	2
Range	1–9
Lymph node regions with metastases at salvage LAE	
N	75
Median	1
Range	0–4

*Not available in 12 cases.
†Not available in 1 case.
iPSA = initial PSA concentration; ISUP = International Society of Urological Pathology; RPE = radical prostatectomy; PSA = prostate-specific antigen; LAE = lymphadenectomy.
Data in parentheses are percentages unless otherwise specified.

(difference in areas under the ROC curves, 0.222; 95% CI, 0.147–0.298; $P < 0.001$).

On the template-based analysis, specificity was 93.3% (95% CI, 85.9%–97.0%) and 100% (95% CI, not available) for ^{18}F-rhPSMA-7 and ^{18}F-rhPSMA-7.3 PET and morphologic imaging, respectively. ^{18}F-rhPSMA-7 and ^{18}F-rhPSMA-7.3 PET detected lymph node metastases in 61 of 75 histopathologically proven metastatic lymph node template regions (sensitivity, 81.3%; 95% CI, 70.1%–89.0%) whereas morphologic imaging was positive in only 9 of 75 lymph node templates (sensitivity, 12.0% 95% CI, 6.3%–21.6%). The PPV was 92.4% for ^{18}F-rhPSMA-7 and ^{18}F-rhPSMA-7.3 PET and 100% for morphologic imaging. The diagnostic accuracy was 87.3% (95% CI, 80.5%–92.0%) for ^{18}F-rhPSMA-7 and ^{18}F-rhPSMA-7.3 PET and 64.5% (95% CI, 47.2%–64.5%) for morphologic imaging (Table 2).

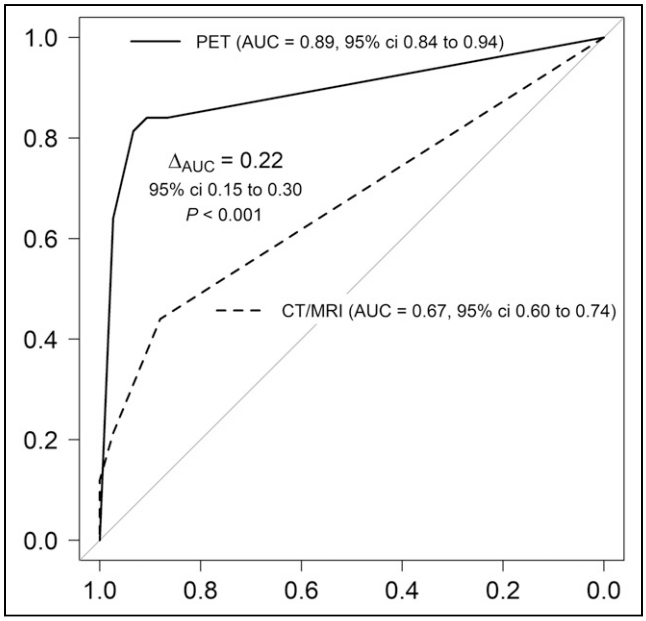

FIGURE 1. Template-based ROC curves for combined data of ^{18}F-rhPSMA-7 and ^{18}F-rhPSMA-7.3 PET (black line) and morphologic imaging (CT/MRI) (dotted line) for assessment of lymph node metastases in all 150 lymph node regions. AUC = area under the curve.

In detail, 75 template regions were free of tumor invasion after histopathologic evaluation, with 70 of them being correctly identified as negative with PET and 75 of them being correctly identified as negative with morphologic imaging. Five template regions (in 3 patients) were classified as suspicious on PET, with no correlation on histopathology (false-positive), whereas morphologic imaging resulted in no template regions being judged as false positive. Follow-up was available in 2 of the patients with false-positive results on PET with slightly increasing PSA levels after surgery but no sign of metastasis in the follow-up ^{18}F-rhPSMA-7 and ^{18}F-rhPSMA-7.3 PET scan.

Fourteen template regions were false-negative on PET, whereas 66 template regions resulted in a false-negative finding on morphologic imaging. Data for the patient-based analysis are presented in Supplemental Table 3. A separate analysis of ^{18}F-rhPSMA-7 and ^{18}F-rhPSMA-7.3 is presented in Supplemental Table 4; in this table, ^{18}F-rhPSMA-7 and ^{18}F-rhPSMA-7.3 PET presented with a similar PPV (92.3% for ^{18}F-rhPSMA-7 and 92.5% for ^{18}F-rhPSMA-7.3).

Uptake in ^{18}F-rhPSMA-7 and ^{18}F-rhPSMA-7.3 PET and Lesion Size

The mean SUV_{max} of histologically confirmed pelvic lymph node metastases rated as suspicious on PET was 16.7 ± 24.7 (range,

TABLE 2
Template-Based Analysis

^{18}F-rhPMSA-7.3 PET/CT rating	Histology: lymph node metastasis		Proportions
	Positive	Negative	
Combined data for ^{18}F-rhPSMA-7 and ^{18}F-rhPSMA-7.3			
Positive	61	5	PPV: 92.4% (95% CI, 83.3%–96.8%)
Negative	14	70	NPV: 83.3% (95% CI, 72.2%–90.6%)
Total	75	75	150
	Sensitivity: 81.3% (95% CI, 70.1%–89.0%)	Specificity: 93.3% (95% CI, 85.9%–97.0%)	Accuracy: 87.3% (95% CI, 80.5–92.0)
Morphologic imaging (CT/MRI)			
Positive	9	0	PPV: 100% (95% CI, N/A)
Negative	66	75	NPV: 53.2% (95% CI, 44.5%–61.6%)
Total	75	75	150
	Sensitivity: 12.0% (95% CI, 6.3%–21.6%)	Specificity: 100% (95% CI, N/A)	Accuracy: 64.5% (95% CI, 47.2%–64.5%)

Scores ≥ 4 in PET and morphologic imaging rated positive.
NPV = negative predictive value; N/A = not available as cannot be calculated (there exists no CI for point estimator of 1 in a generalized estimating equation).

3.3–146.6). The corresponding mean lesion size of these PET-positive, histologically confirmed lymph nodes was 6.3 ± 3.1 mm (range, 2–15 mm). The mean size of histologically confirmed lymph nodes rated as suspicious on morphologic imaging was 10.6 ± 2.7 mm (range, 7–15 mm). The mean size of histologically confirmed lymph nodes not rated as suspicious on morphologic imaging was 5.3 ± 2.3 mm (range, 2–14 mm).

A representative example of a correctly classified lymph node metastases by PET/CT is shown in Figure 2.

DISCUSSION

The value of PSMA PET for imaging patients with recurrence of PC after primary treatment has been extensively reported (*5,6,20, 27–29*). Here, we reviewed real-world clinical data supporting the utility of the novel PSMA-targeting radiopharmaceuticals ^{18}F-rhPSMA-7 and ^{18}F-rhPSMA-7.3. To date, the efficacy of both ^{18}F-rhPSMA-7 and ^{18}F-rhPSMA-7.3 for imaging PC patients has been demonstrated by several retrospective studies (*15,16,30*), including their high accuracy for lymph node staging in patients with primary PC (*22,31*). The presented data demonstrate a high specificity and PPV of ^{18}F-rhPSMA-7 and ^{18}F-rhPSMA-7.3 PET for lymph node metastases in patients with recurrent PC after radical prostatectomy validated by histopathology. On a template-based analysis, ^{18}F-rhPSMA-7.3 offers a higher accuracy and sensitivity than morphologic imaging.

These results are in line with a similar, histopathologically validated analysis using ^{68}Ga-PSMA-11 that showed a sensitivity, specificity, and PPV of 77.9%, 97.3%, and 94.6%, respectively, compared with 81.3%, 93.3%, and 92.4% in our analysis, respectively (*5*). Further, the difference in the areas under the receiver-operating-characteristic curves for morphologic images was 0.139 with ^{68}Ga-PSMA-11 compared with 0.222 with ^{18}F-rhPSMA-7 and ^{18}F-rhPSMA-7.3 in our analysis (*5*). Similar to ^{68}Ga-PSMA-11 PET, our data show

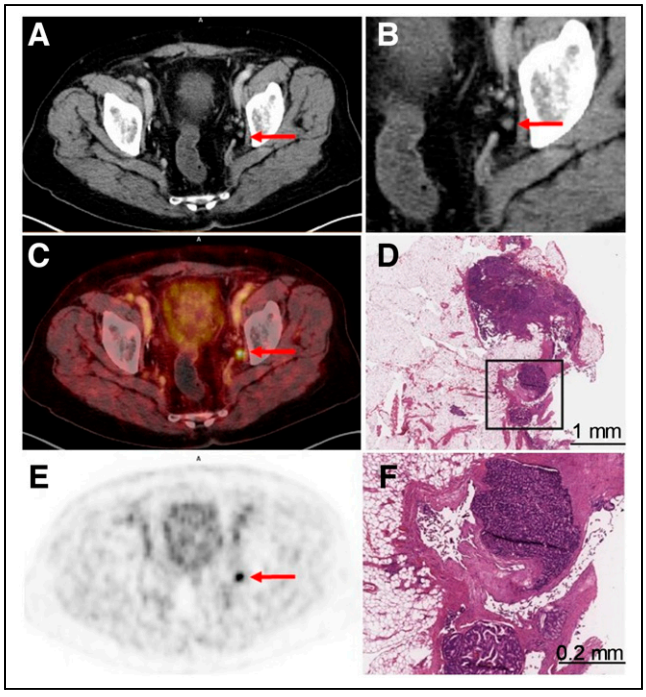

FIGURE 2. A 75-y-old patient with biochemical recurrence after radical prostatectomy (ISUP grade group 4, pT3b pN0 cM0, iPSA level: 11 ng/mL, PSA level at time of PET examination: 1.02 ng/mL) and a correctly classified lymph node metastasis by ^{18}F-rhPSMA-7.3 PET. A morphologically nonsuspicious lymph node, 5 mm in diameter, is visible in left obturator fossa on CT (A and B) that shows intense, focal and suggestive tracer uptake in ^{18}F-rhPSMA-7.3 PET and fused PET/CT (C and E). Salvage lymphadenectomy with histologic evaluation confirmed a single lymph node metastasis (D and F). Arrow shows lymph node metastasis. iPSA = initial PSA concentration; ISUP = International Society of Urological Pathology.

that these novel tracers can detect small lymph node metastasis (a lesion size smaller than 10 mm) in the recurrent PC setting (*5*). Salvage lymph node surgery represents a therapeutic option for patients experiencing biochemical recurrence after radical prostatectomy, and previous ^{11}C-choline PET–guided data suggest that up to 40% of patients may experience recurrence-free survival after PET-guided salvage lymph node dissection (*32*). More recently, Horn et al. showed that in a subgroup of patients with recurrent PC undergoing PSMA PET–guided salvage surgery, complete biochemical response was achieved in 66% of patients (*2*). Moreover, it is believed that PET-guided salvage lymph node dissection may prolong the time until initiation of hormonal treatment, which is associated with significant morbidity (*33,34*). For salvage surgery with potential complications, a high specificity and PPV are of utmost importance to avoid unnecessary interventions. Interestingly, the specificity of morphologic imaging on a template base was also excellent, which is most likely related to the strict criteria for the determination of metastases. However, as known from the literature, the sensitivity of morphologic imaging is rather low as it can detect only lymph node metastases with already enlarged (>10 mm) lesions.

The pure enantiomeric form of ^{18}F-rhPSMA-7, ^{18}F-rhPSMA-7.3, has been selected as the lead rhPSMA compound for clinical development on the basis of preclinical assessments showing favorable safety and kinetic profiles for diagnostic imaging of PC (*14,18*). Because of the limited numbers, no sound comparison of the diagnostic performance of ^{18}F-rhPSMA-7 versus ^{18}F-rhPSMA-7.3 is possible in the present study. However, we note similar PPVs for the 2 compounds, which is the only descriptive statistical value to be unaffected by the potential selection bias that results from the present study design. Another limitation of this retrospective analysis is its potential selection bias due to the selection of patients and the lymph node template regions to be removed on the basis of the clinical reads of the ^{18}F-rhPSMA-7 and ^{18}F-rhPSMA-7.3 PET scans. Possible imaging-negative nodes could have been missed, which would impact the sensitivity estimate. Therefore, PPV is the only descriptive statistical value independent of this bias. Of note, specificity on the patient-based analysis was only informed by 4 cases (Supplemental Table 3). For different reasons, it was not always feasible to perform surgery shortly after PET examination (median time between PET and surgery, 59 d; range, 19–117 d). Thus, in principle, it cannot be excluded that there was tumor progression or even new tumor lesions at the time of surgery. The data presented in the supplemental materials for separate analyses of ^{18}F-rhPSMA-7 and ^{18}F-rhPSMA-7.3 should be interpreted with caution given the limited number of patients in each group. Further prospective studies with ^{18}F-rhPSMA-7.3 are warranted to confirm the diagnostic accuracy for lymph node staging and to avoid potential bias.

CONCLUSION

^{18}F-rhPSMA-7 and ^{18}F-rhPSMA-7.3 PET are superior to morphologic imaging for detecting pelvic lymph node metastases and helping guide salvage lymph node surgery. They offer a high PPV, comparable to that reported for ^{68}Ga-PSMA-11, while yielding the benefits of a radiofluorinated tracer such as the potential for scale production and wide-range distribution.

DISCLOSURE

Hans-Jürgen Wester, Alexander Wurzer, and Matthias Eiber have a patent application for rhPSMA. Hans-Jürgen Wester and Matthias Eiber received funding from Blue Earth Diagnostics Ltd. (Oxford, U.K., Licensee for rhPSMA) as part of an academic collaboration. Matthias Eiber reports prior consulting activities for Blue Earth Diagnostics Ltd., Novartis, Telix, Progenics, Bayer, Point Biopharma, and Janssen. Hans-Jürgen Wester is founder, shareholder, and advisor board member of Scintomics GmbH (Fuerstenfeldbruck, Germany). Siemens Medical Solutions (Erlangen, Germany) supported the application of Biograph mCT flow as part of an academic collaboration. Tobias Maurer reports prior consulting activities for Blue Earth Diagnostics Ltd., Novartis, Telix, ROTOP Pharma, Advanced Accelerator Applications International S.A., GEMoAb, and Astellas. No other potential conflict of interest relevant to this article was reported.

KEY POINTS

QUESTION: What is the value of the radiopharmaceuticals ^{18}F-rhPSMA-7 and ^{18}F-rhPSMA-7.3 for assessing the presence of lymph node metastases before potential salvage lymphadenectomy?

PERTINENT FINDINGS: This histopathologically validated, retrospective study shows that ^{18}F-rhPSMA-7 and ^{18}F-rhPSMA-7.3 are superior to morphologic imaging and comparable to ^{68}Ga-PSMA-11 for N staging of biochemical recurrent prostate cancer.

IMPLICATIONS FOR PATIENT CARE: ^{18}F-rhPSMA-7 and ^{18}F-rhPSMA-7.3 can detect small soft-tissue metastases with a high, template-based specificity of 93%.

REFERENCES

1. Freedland SJ, Presti JC Jr, Amling CL, et al. Time trends in biochemical recurrence after radical prostatectomy: results of the SEARCH database. *Urology.* 2003;61:736–741.
2. Horn T, Kroenke M, Rauscher I, et al. Single lesion on prostate-specific membrane antigen-ligand positron emission tomography and low prostate-specific antigen are prognostic factors for a favorable biochemical response to prostate-specific membrane antigen-targeted radioguided surgery in recurrent prostate cancer. *Eur Urol.* 2019;76:517–523.
3. Bandini M, Fossati N, Briganti A. Salvage surgery for nodal recurrent prostate cancer. *Curr Opin Urol.* 2017;27:604–611.
4. Steuber T, Jilg C, Tennstedt P, et al. Standard of care versus metastases-directed therapy for PET-detected nodal oligorecurrent prostate cancer following multimodality treatment: a multi-institutional case-control study. *Eur Urol Focus.* 2019;5:1007–1013.
5. Rauscher I, Maurer T, Beer AJ, et al. Value of ^{68}Ga-PSMA HBED-CC PET for the assessment of lymph node metastases in prostate cancer patients with biochemical recurrence: comparison with histopathology after salvage lymphadenectomy. *J Nucl Med.* 2016;57:1713–1719.
6. Maurer T, Gschwend JE, Rauscher I, et al. Diagnostic efficacy of ^{68}Gallium-PSMA positron emission tomography compared to conventional imaging for lymph node staging of 130 consecutive patients with intermediate to high risk prostate cancer. *J Urol.* 2016;195:1436–1443.
7. Eder M, Schafer M, Bauder-Wust U, et al. ^{68}Ga-complex lipophilicity and the targeting property of a urea-based PSMA inhibitor for PET imaging. *Bioconjug Chem.* 2012;23:688–697.
8. Afshar-Oromieh A, Malcher A, Eder M, et al. PET imaging with a [^{68}Ga]gallium-labelled PSMA ligand for the diagnosis of prostate cancer: biodistribution in humans and first evaluation of tumour lesions. *Eur J Nucl Med Mol Imaging.* 2013;40:486–495.
9. Perera M, Papa N, Christidis D, et al. Sensitivity, specificity, and predictors of positive ^{68}Ga-prostate-specific membrane antigen positron emission tomography in advanced prostate cancer: a systematic review and meta-analysis. *Eur Urol.* 2016;70:926–937.
10. Cornford P, Bellmunt J, Bolla M, et al. EAU-ESTRO-SIOG guidelines on prostate cancer. Part II: Treatment of relapsing, metastatic, and castration-resistant prostate cancer. *Eur Urol.* 2017;71:630–642.

11. Fendler WP. Assessment of ^{68}Ga-PSMA-11 PET accuracy in localizing recurrent prostate cancer: a prospective single-arm clinical trial. *JAMA Oncol.* 2019;5:856–863.
12. Oh SW, Wurzer A, Teoh EJ, et al. Quantitative and qualitative analyses of biodistribution and PET image quality of novel radiohybrid PSMA, ^{18}F- rhPSMA-7, in patients with prostate cancer. *J Nucl Med.* 2020;61:702–709.
13. Wurzer A, DiCarlo D, Schmidt A, et al. Radiohybrid ligands: a novel tracer concept exemplified by ^{18}F- or ^{68}Ga-labeled rhPSMA-inhibitors. *J Nucl Med.* 2020;61:735–742.
14. Wurzer A, Parzinger M, Konrad M, et al. Preclinical comparison of four [^{18}F, ^{nat}Ga]rhPSMA-7 isomers: influence of the stereoconfiguration on pharmacokinetics. *EJNMMI Res.* 2020;10:149.
15. Rauscher I, Karimzadeh A, Schiller K, et al. Detection efficacy of ^{18}F-rhPSMA-7.3 PET/CT and impact on patient management in patients with biochemical recurrence of prostate cancer after radical prostatectomy and prior to potential salvage treatment. *J Nucl Med.* 2021;62:1719–1726.
16. Eiber M, Kronke M, Wurzer A, et al. ^{18}F-rhPSMA-7 positron emission tomography for the detection of biochemical recurrence of prostate cancer following radical prostatectomy. *J Nucl Med.* 2020;61:696–701.
17. Wurzer A, Di Carlo D, Herz M, et al. Automated synthesis of [^{18}F]Ga-rhPSMA-7/-7.3: results, quality control and experience from more than 200 routine productions. *EJNMMI Radiopharm Chem.* 2021;6:4.
18. Tolvanen T, Kalliokoski KK, Malaspina S, et al. Safety, biodistribution and radiation dosimetry of ^{18}F-rhPSMA-7.3 in healthy adult volunteers. *J Nucl Med.* 2021;62:679–684.
19. Souvatzoglou M, Eiber M, Martinez-Moeller A, et al. PET/MR in prostate cancer: technical aspects and potential diagnostic value. *Eur J Nucl Med Mol Imaging.* 2013;40(suppl 1):S79–S88.
20. Eiber M, Maurer T, Souvatzoglou M, et al. Evaluation of hybrid ^{68}Ga-PSMA ligand PET/CT in 248 patients with biochemical recurrence after radical prostatectomy. *J Nucl Med.* 2015;56:668–674.
21. Rausch I, Cal-Gonzalez J, Dapra D, et al. Performance evaluation of the Biograph mCT Flow PET/CT system according to the NEMA NU2-2012 standard. *EJNMMI Phys.* 2015;2:26.
22. Kroenke M, Wurzer A, Schwamborn K, et al. Histologically-confirmed diagnostic efficacy of ^{18}F-rhPSMA-7 positron emission tomography for N-staging of patients with primary high risk prostate cancer. *J Nucl Med.* 2020;61:710–715.
23. Obuchowski NA. Nonparametric analysis of clustered ROC curve data. *Biometrics.* 1997;53:567–578.
24. The R project for statistical computing. The R project website. https://www.R-project.org/. Accessed September 14, 2022.
25. Robin X, Turck N, Hainard A, et al. pROC: an open-source package for R and S+ to analyze and compare ROC curves. *BMC Bioinformatics.* 2011;12:77.
26. Højsgaard S, Halekoh U, Yan J. The R package geepack for generalized estimating equations. *J Stat Softw.* 2005;15:1–11.
27. Afshar-Oromieh A, Avtzi E, Giesel FL, et al. The diagnostic value of PET/CT imaging with the ^{68}Ga-labelled PSMA ligand HBED-CC in the diagnosis of recurrent prostate cancer. *Eur J Nucl Med Mol Imaging.* 2015;42:197–209.
28. Hijazi S, Meller B, Leitsmann C, et al. Pelvic lymph node dissection for nodal oligometastatic prostate cancer detected by ^{68}Ga-PSMA-positron emission tomography/computerized tomography. *Prostate.* 2015;75:1934–1940.
29. Herlemann A, Wenter V, Kretschmer A, et al. ^{68}Ga-PSMA positron emission tomography/computed tomography provides accurate staging of lymph node regions prior to lymph node dissection in patients with prostate cancer. *Eur Urol.* 2016;70:553–557.
30. Chantadisai M, Buschner G, Kronke M, et al. Positive predictive value and correct detection rate of ^{18}F-rhPSMA-7 PET in biochemically recurrent prostate cancer validated by composite reference standard. *J Nucl Med.* 2021;62:968–974.
31. Langbein T, Kroenke M, Rauscher I, et al. Preliminary data on the diagnostic efficacy of F-18-rhPSMA-7.3 PET imaging for N-staging of patients with intermediate and high-risk prostate cancer compared to histopathology [abstract]. *J Nucl Med.* 2020;61(suppl 1):1267.
32. Suardi N, Gandaglia G, Gallina A, et al. Long-term outcomes of salvage lymph node dissection for clinically recurrent prostate cancer: results of a single-institution series with a minimum follow-up of 5 years. *Eur Urol.* 2015;67:299–309.
33. Saigal CS, Gore JL, Krupski TL, et al. Androgen deprivation therapy increases cardiovascular morbidity in men with prostate cancer. *Cancer.* 2007;110:1493–1500.
34. Tsai HK, D'Amico AV, Sadetsky N, Chen MH, Carroll PR. Androgen deprivation therapy for localized prostate cancer and the risk of cardiovascular mortality. *J Natl Cancer Inst.* 2007;99:1516–1524.